

Characterization of m-GaN and a-GaN Crystallographic Planes after Being Chemically Etched in TMAH Solution

Nedal Al Taradeh, Eric Frayssinet, Christophe Rodriguez, Frédéric Morancho, Camille Sonneville, Luong-Viet Phung, Ali Soltani, Florian Tendille, Yvon Cordier, Hassan Maher

▶ **To cite this version:**

Nedal Al Taradeh, Eric Frayssinet, Christophe Rodriguez, Frédéric Morancho, Camille Sonneville, et al.. Characterization of m-GaN and a-GaN Crystallographic Planes after Being Chemically Etched in TMAH Solution. Energies, 2021, 14 (14), pp.4241. 10.3390/en14144241 . hal-03452669

HAL Id: hal-03452669
https://cnrs.hal.science/hal-03452669

Submitted on 27 Nov 2021

HAL is a multi-disciplinary open access archive for the deposit and dissemination of scientific research documents, whether they are published or not. The documents may come from teaching and research institutions in France or abroad, or from public or private research centers.

L'archive ouverte pluridisciplinaire **HAL**, est destinée au dépôt et à la diffusion de documents scientifiques de niveau recherche, publiés ou non, émanant des établissements d'enseignement et de recherche français ou étrangers, des laboratoires publics ou privés.

energies

MDPI

Article

Characterization of m-GaN and a-GaN Crystallographic Planes after Being Chemically Etched in TMAH Solution

Nedal Al Taradeh [1,*], Eric Frayssinet [2], Christophe Rodriguez [1], Frederic Morancho [3], Camille Sonneville [4], Luong-Viet Phung [4], Ali Soltani [1], Florian Tendille [5], Yvon Cordier [2] and Hassan Maher [1]

1 Laboratoire Nanotechnologies Nanosystèmes, CNRS UMI-3463, 3IT, Université de Sherbrooke, Sherbrooke, QC J1K OA5, Canada; Christophe.Rodriguez@USherbrooke.ca (C.R.); ali.soltani@usherbrooke.ca (A.S.); hassan.maher@usherbrooke.ca (H.M.)
2 University Côte d'Azur, CNRS (Centre National de la Recherche Scientifique), CRHEA (Centre de Recherche sur l'Hétéro-Epitaxie et ses Applications), rue Bernard Grégory, 06560 Valbonne, France; ef@crhea.cnrs.fr (E.F.); yc@crhea.cnrs.fr (Y.C.)
3 Laboratoire d'Analyse et d'Architecture des Systèmes (LAAS-CNRS), Université de Toulouse, CNRS, Av du Colonel Roche, BP 54200, 31031 Toulouse, France; morancho@laas.fr
4 INSA Lyon, Université Claude Bernard Lyon 1, Ecole Centrale de Lyon, CNRS, Ampère, UMR5005, 69621 Villeurbanne, France; camille.sonneville@insa-lyon.fr (C.S.); luong-viet.phung@insa-lyon.fr (L.-V.P.)
5 Saint-Gobain, 12 Place de l'Iris, 92400 Courbevoie, France; Florian.Tendille@saint-gobain.com
* Correspondence: nedal.al.taradeh@usherbrooke.ca

Abstract: This paper proposes a new technique to engineer the Fin channel in vertical GaN FinFET toward a straight and smooth channel sidewall. Consequently, the GaN wet etching in the TMAH solution is detailed; we found that the m-GaN plane has lower surface roughness than crystallographic planes with other orientations, including the a-GaN plane. The grooves and slope (Cuboids) at the channel base are also investigated. The agitation does not assist in Cuboid removal or crystallographic planes etching rate enhancement. Finally, the impact of UV light on m and a-GaN crystal plane etching rates in TMAH has been studied with and without UV light. Accordingly, it is found that the m-GaN plane etching rate is enhanced from 0.69 to 1.09 nm/min with UV light; in the case of a-GaN plane etching, UV light enhances the etching rate from 2.94 to 4.69 nm/min.

Keywords: vertical GaN FinFET; GaN etching; UV light; Tetramethylammonium hydroxide (TMAH); ICP-RIE dry etching; channel sidewall engineering

check for updates

Citation: Al Taradeh, N.; Frayssinet, E.; Rodriguez, C.; Morancho, F.; Sonneville, C.; Phung, L.-V.; Soltani, A.; Tendille, F.; Cordier, Y.; Maher, H. Characterization of m-GaN and a-GaN Crystallographic Planes after Being Chemically Etched in TMAH Solution. *Energies* **2021**, *14*, 4241. https://doi.org/10.3390/en14144241

Academic Editors: Julien Buckley, René Escoffier and Matthew Charles

Received: 5 June 2021
Accepted: 8 July 2021
Published: 14 July 2021

Publisher's Note: MDPI stays neutral with regard to jurisdictional claims in published maps and institutional affiliations.

Copyright: © 2021 by the authors. Licensee MDPI, Basel, Switzerland. This article is an open access article distributed under the terms and conditions of the Creative Commons Attribution (CC BY) license (https://creativecommons.org/licenses/by/4.0/).

1. Introduction

As a wide-bandgap transistor technology, GaN provides a compelling opportunity to achieve unprecedented performance levels and efficiency in power electronics systems, owing to its large breakdown electric field and high Baliga's Figure of merit [1–4]. It guarantees a 10% reduction of losses in power conversion circuits [5]. Further, it also offers faster, cooler and smaller power devices than its silicon counterparts [6,7].

Thus far, both lateral and vertical structures have been considered to be incorporated in the GaN power devices [8]. The GaN-based high electron mobility transistor (HEMT) device's immense potential comes from the high density, the high electron mobility in the 2-dimensional electron gas (2DEG) formed at its heterostructure [9]. However, with the high electric field close to the device surface, the high current density along the 2D channel generates significant heat, increasing the device access resistance and incidences of current collapse due to traps [10,11]. Contrariwise, the vertical GaN power devices, especially the GaN FinFET, have garnered considerable attention because of their potential to reach high voltage and high output current density [12,13]. Furthermore, they exhibit superior thermal performance compared to lateral devices [14]. The first design and fabrication of a Normally-Off GaN vertical fin power FET (or MOSVFET) have been reported by W. Li et al. [15]. They first used a TCAD tool to investigate the impact of the main critical

parameters on the device performance, such as the bulk GaN mobility, the gate-to-gate distance, and the gate length. They achieved an ON-state resistance (R_{ON}) of 2.8 mΩ·cm^2 and a breakdown voltage (V_{BR}) of 1.2 kV. Several prototype versions of GaN FinFET devices fabricated on GaN or a foreign substrate have been published in the literature [16–18].

The vertical GaN FinFET fabrication process begins with the anisotropic GaN etching, executed by dry Induced Coupled Plasma-Reactive Ion Etching (ICP-RIE) [19]. However, the main drawback of such technology is the GaN sidewall surface's damage with difficulty in obtaining straight etched sidewalls [20]. Engineering the Fin channel sidewalls plays a crucial role in the electrical performance of vertical GaN FinFET devices [21]. Therefore, it is vital to optimize a smoothing process after dry etching to remove the channel sidewalls imperfections and the GaN/dielectric interface of the device is therefore improved.

For vertical GaN FinFET devices, a Fin channel structure with non-polar plane side walls is favorable for Normally-Off operation. Non-polar planes at the FinFET channel's sidewall are suitable for fabricating the Normally-Off device. Depending on the channel width, a low quantity of charge can be present in the channel at V_{GS} = 0 V [22,23]. The m-GaN and a-GaN channel sidewalls revealing process require a specific lithography orientation of the Fin channel structure [24]. The chemical etching process has also been demonstrated in the literature for post dry etching treatment of GaN [25–28].To achieve this, Tetramethylammonium hydroxide (TMAH) is widely used [29,30]. Furthermore, UV light-based TMAH etching is also effective technique to enhance the GaN sidewall's etching rate [31]. It also improves the etching selectivity when a dielectric material is used as a mask [32,33].

Since GaN chemical etching is a crystallographic dependent process, the Fins sidewalls should be precisely aligned to the crystal plane that we would like to reveal after etching. Therefore, for GaN coupons processing, developing a sensitive orientation determination procedure is an essential step.

The purpose of this paper is to investigate one of the most critical steps in the fabrication process of vertical GaN FinFET transistors, which is the etching of the channel sidewalls. An Orientation Determination (OD) technique has also been demonstrated for GaN Fin channel sidewall. Finally, this work presents a procedure to improve the GaN transistor fabrication process and therefore the performance of the device.

2. Experiment Technique

In this study, we intend to determine the exact orientation of the a-GaN and m-GaN planes on the coupon samples, followed by investigating the GaN crystallographic etching with TMAH solution. The GaN channel fingers are firstly fabricated using the top-down process. The wet etching has been used to reveal the crystallographic planes on the channel sidewalls. The fabrication process has been depicted in Figure 1. A 7 µm thick GaN epi-layer wafer (Sample1) grown by Metal-Organic Chemical Vapor Deposition (MOCVD) on Sapphire substrate is used for this experiment. The size of this square sample is 1 cm × 1 cm. For this purpose, 180 fingers with 15 × 2 µm^2 dimensions oriented from 0° to 180° with a step of 1° are fabricated (Figures 1 and 2).

The fabrication process starts with the deposition of a 1 µm thick SiO_2 (PECVD) layer on the wafer to act as a mask. An e-beam lithography is then performed with PMMA 9% resist for finger definition. The SiO_2 is etched using dry etching with CF4/He gas mixture to transfer the pattern from the resist to the SiO2 mask. This step is followed by the ICP-RIE using Cl2/Ar gas mixture for etching a 2 µm of GaN for the Fins formation and, finally, the GaN wet etching is performed using TMAH solution. For this last point, the recipe mainly consists of TMAH 25% heated in glassware for (80–85 °C) temperature range with UV-assisted source. It is worth mentioning that GaN wafers de-oxidation using (1:10) diluted HCl solution before any TMAH wet etching step is very important because it will prepare the GaN surface for the etching process [34].

The Scanning Electron Microscope (SEM) characterization for the m-GaN oriented finger is shown in Figure 2.

The finger shape after ICP-RIE dry etching is shown in Figure 2a, while the shape of the same finger after chemical etching is presented in Figure 2b. Figure 2c presents an ensemble of fingers after ICP-RIE. The GaN crystallographic planes are shown in Figure 2d.

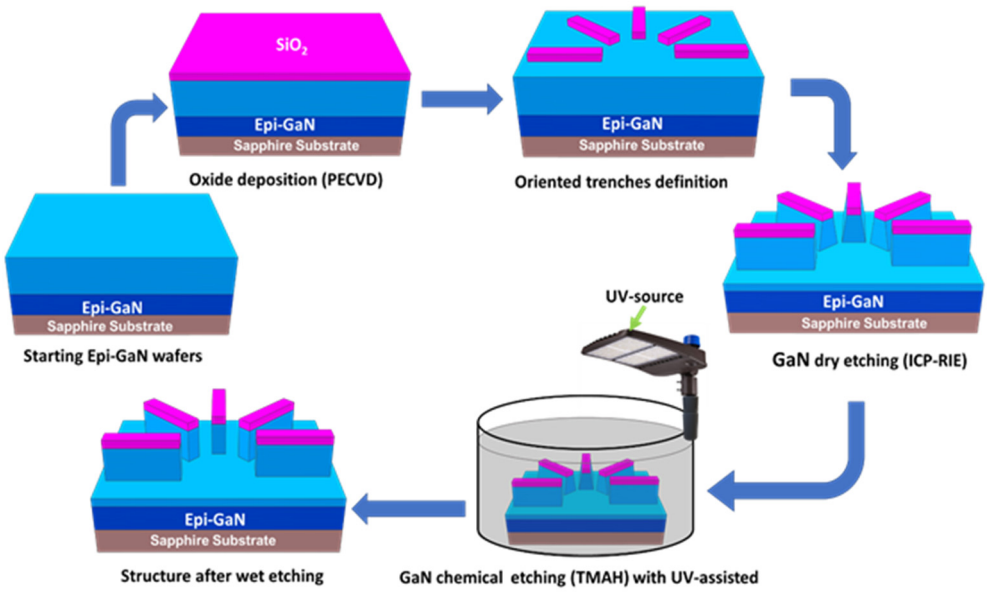


Figure 1. The fabrication process of GaN's fingers for sidewalls engineering.

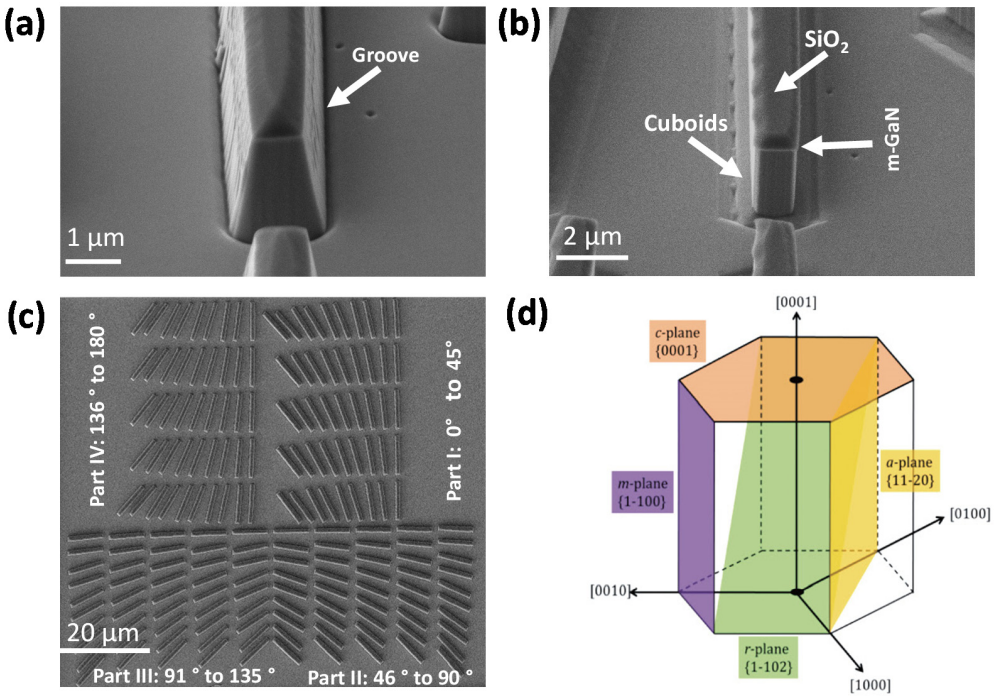


Figure 2. SEM images of fingers after GaN etching;(**a**) bird eye view of finger after dry etching; (**b**) bird eye view of finger after wet etching with TMAH solution; (**c**) top view of an ensemble of fingers for orientation between 0° and 180°; (**d**) GaN crystallographic planes [33].

Following the previous experiments, another sample (Sample 2) grown on GaN substrate was also processed. Indeed, a coupon having the same epitaxial layers as Sample1 has been processed. In this coupon, the SiO_2 mask for the GaN etching is replaced by the

Ti/Au/Ni metal stack with 20 nm/350 nm/30 nm thicknesses, respectively, deposited by the e-beam evaporation. The studied patterns have a star shape consisting of 24 identical Fins fingers with 250 nm width and 2.3 µm thickness shifted from each other with 15°. The same fabrication process depicted in Figure 1 has been used to fabricate the Fins fingers, except for the mask, which is metallic here in this second experiment. The vertical fingers of the star pattern were aligned on the m-GaN plane. The m-GaN and a-GaN crystal planes are investigated during the etching with TMAH.

The fabrication procedure shown in Figure 1 has been associated with some challenges and limitations. For instance, optimizing e-beam lithography, initialization of the GaN surface before the TMAH etching, or selecting a source metal stack compatible with all fabrication steps are just a few of them. Indeed, to determine the metal stack that will be suitable for the device fabrication process, several tests have been performed. Likewise, the selected metal stack should present no contamination for the PECVD, ALD and ICP-RIE machines. Finally, Cr/Au/Cr metal stack has been considered most viable for fabricating the real device. This metal stack will be used for the fabrication of GaN vertical devices.

3. Results and Discussion

The results and discussion section are divided into three main parts. Firstly, SEM has been used to characterize the fabricated structures after wet etching. Both Atomic Force Microscopy (AFM) and SEM are then used to investigate the groove's etching profile in the second part. Finally, the fabrication of vertical GaN channel fingers using the proposed orientation determination has been characterized and discussed.

3.1. GaN Channel Sidewalls Etching Using the Proposed OD Procedure

Sample1 has been dived in TMAH solution for different etching time intervals with a total of 30 min etching time. The channel fingers have been characterized after each etching step to track the sidewall morphology evolution. The six m-GaN's crystal planes and six a-GaN crystal planes (a-GaN planes and m-GaN planes are perpendicular to each other) are investigated. In the case of GaN on sapphire wafer, the flat zone is pre-aligned to the a-GaN plane; therefore, m-GaN planes are located approximatively perpendicularly to the flat. In our fabricated structure, the range of investigated angles was between 0° and 180° with a step of 1°. Therefore, we have investigated all m-GaN and a-GaN planes with ±1°degree precision to estimate the exact GaN crystal orientation. The channel fingers oriented on m-GaN and a-GaN planes have been characterized using SEM after 30 min of chemical etching in TMAH solution, as shown in Figure 3.

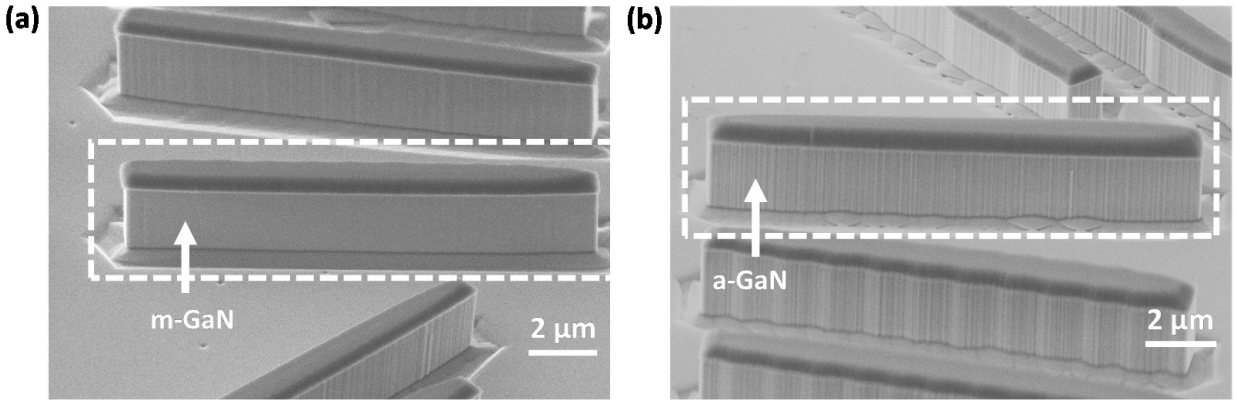


Figure 3. SEM images for m-GaN and a-GaN sidewalls after 30 min in TMAH solution; (**a**) m-GaN sidewall; (**b**) a-GaN sidewall.

It can be easily observed from Figure 3a that the m-GaN plane surrounded by the dashed rectangle has relatively much lower roughness on its surface compared to the a-GaN plane, which is presented in Figure 3b surrounded by the dashed rectangle. After 10 min

of wet etching, the a-GaN plane sidewalls are completely vertical, no further smoothening occurs after that. The relatively higher etching rate of the a-GaN plane results from its lower etching resistivity. On the other hand, a 25 min wet etching process is needed to achieve vertical m-GaN fingers, owing to its higher etching resistivity [35]. In light of this, m-GaN orientated Fins is the best choice for the fabrication of high performance vertical FinFET GaN transistor. Noteworthy is the fact that the etching rate of GaN is not solely determined by TMAH solution parameters; rather, it is determined by a variety of factors, such as the mask selection [36], the doping level [37] and the crystalline quality resulting from GaN epitaxial growth conditions [28].

3.2. Investigation of the Morphology of the Groove Surrounding the Fins after TMAH Etching

It is well known that after the plasma etching, an over-etch appears at the periphery of the patterns (trenching effect) [36]. In our case here, this over-etch creates a groove at the bottom of the Fins. The grooves evolution in both finger sides has been investigated before and after chemical etching. The groove depth was about 94 nm before wet etching. GaN wet etching has been carried out in TMAH for around 120 min in several steps using the same etching recipe. The c-plane is ultimately stable in TMAH solution with only around 2 nm etching depth after 120 min of chemical etching. These 2 nm are resulting from several de-oxidation of GaN surface before TMAH etching between two etching times. Those results are in good agreement with the one obtained by B. Leung et al. and E. Schubert et al., respectively [35,36].

The Cuboid structure characterized by the slope α as in Figure 4b was also investigated. This slope located at the finger base appeared in all our experiments. This structure has also been widely addressed in the literature, as in [37–39]. A clear convincing explanation of the origin of these Cuboids has not been reported yet. Accordingly, one of the reported explanations declaring that the semipolar r crystal plane <**1$\bar{1}$01**> could represent the slope a of the Cuboid The slope angle of the cuboids in our case is 68° after the wet etching. This value is different from the r plane, which is 58° [40].

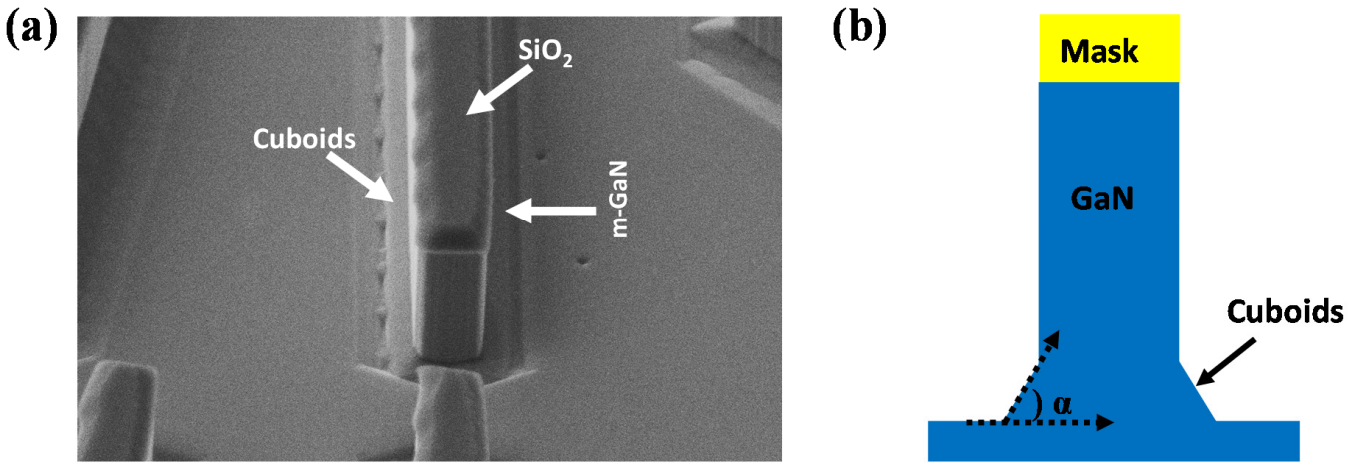


Figure 4. Groove formation due to the GaN etching; (**a**) This work; (**b**) description of cuboids formation.

Another explanation has been reported by Fatahilah, M.F. et al. [30]. According to their observation, the slope is created due to TMAH hydrodynamics flow during the GaN chemical etching. To validate this assumption, we have used two GaN on sapphire substrate samples with dry-etched GaN fingers fabricated using the same process as in Figure 1. Indeed, using the TMAH etching recipe described above, both samples are etched for 25 min, one with agitation and the other without. The TMAH hydrodynamics flow is different for these two samples. After etching, the slopes α observed at the bottom of the fingers are identical on both samples. Furthermore, the Cuboids slope is not depending on the distance between the two neighbor fingers. Thus, the origin of the Cuboids created

at the Fins GaN sidewall base after TMAH etching is still not elucidated and needs to be more investigated.

On the other hand, the impact of UV-light on Cuboids etching has also been investigated by diving two GaN on GaN wafers for 30 min in a TMAH solution, one with and one without UV assistance. The Fin patterns from both wafers have been observed before and after etching using the SEM. It is found that the cuboid shape is the same for both samples, which is a proof that the UV-light is not impacting the cuboid formation.

3.3. GaN Non-Polar Planes Wet Etching Rate Estimation in TMAH Solution with and without UV Source Utilization

The proposed OD technique has been used to determine exactly m-GaN oriented vertical GaN channel fingers using the top-down approach. The used wafer is a thick GaN grown layer on GaN substrate with 1 cm × 1 cm dimensions. This sample comes from a 2 inches wafer where the flat zone is aligned to the GaN's m-plane. The processing of this sample started with a pre-alignment step where a pattern comparable to the one presented in Figure 2c is placed at the sample's periphery. All these patterns are etched to reveal the exact m-plane. As in our case, where we usually work on coupons, this pre-alignment procedure is very useful for the GaN-on-GaN wafers since the exact in-plane crystal orientation is not well identified. In these coupons, the m-plane is not precisely defined, since they are diced from a 2 inch wafer. The proposed approach is a simple solution that can be adopted in the device fabrication process to eliminate any miss-alignment of the Fins.

Since the crystal planes can all be identified with a precision of one degree, so the sample can now be processed. The e-beam lithography is used to align the Fins finger to the m-plane revealed on the pre-alignment marks. This sample uses the same metal stack previously used serves as a mask for the GaN etching to define the Fins. After metal deposition and GaN dry etching, the patterns are then ready for the channel sidewall etching step.

To determine how UV light will affect the etching rate for both a-GaN and m-GaN planes, A pair of samples was prepared and then chemically etched in TMAH solution at different time intervals: one was etched using the standard process using UV-light, while the other was etched without UV-light. The lateral etching depth was then measured after each time interval. Figure 5 illustrates the plot of m-GaN and a-GaN etching rates with and without UV-light.

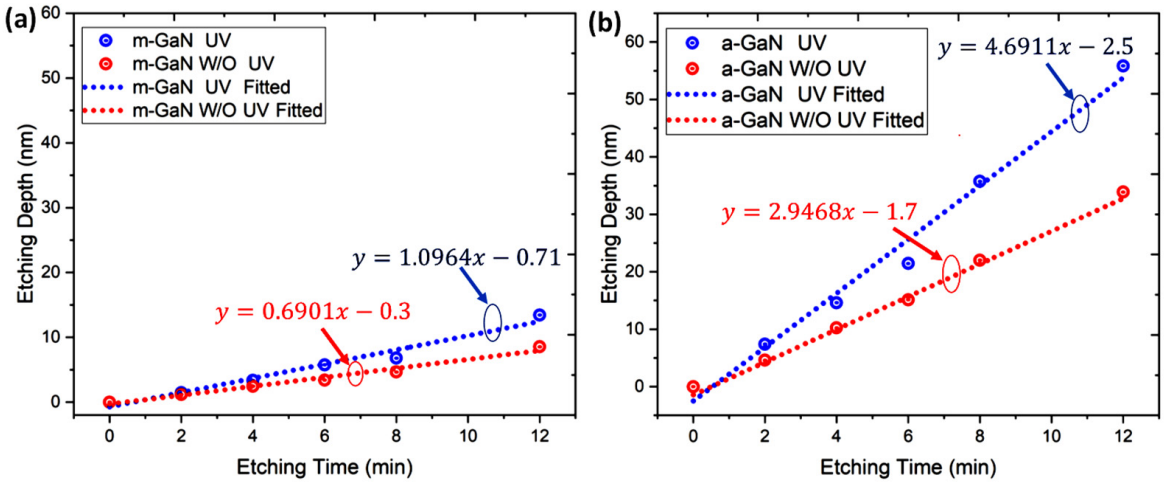


Figure 5. m-GaN and a-GaN wet etching rate in TMAH solution with and without UV-source. (**a**) for m-GaN plane, (**b**) for a-GaN plane.

It is observable from Figure 5 that the m-GaN etching rate is enhanced from 0.69 to 1.1 nm/min by using UV light. Moreover, in the case of a-GaN etching rate, UV light enhances the etching rate from 2.95 to 4.69 nm/min.

After revealing the GaN crystallographic planes, the etching rate will be affected by the etching resistivity of each plane. We have plotted the etching depth for both a-GaN and m-GaN planes during the wet etching using the SEM measurements for etching durations ranging from 2 to 12 min.

In Table 1, we present the obtained results and compare them to those reported in the literature.

Table 1. GaN crystallographic etching rate (β) of m-GaN and a-GaN planes in TMAH for different wet etching setups.

Ref	Authors	Wafer/ Substrate	GaN Wet Etching Recipe	UV Light	Etch Time (min)	Mask	β	
							m-GaN (nm/min)	a-GaN (nm/min)
1	This work	GaN/GaN	TMAH, 25%, 85 °C	Yes	14	Ti/Au/Ni	1.09	4.69
2	This work	GaN/GaN	TMAH, 25%, 85 °C	No	14	Ti/Au/Ni	0.69	2.95
3	B. Leung et al. [35]	GaN/GaN	TMAH, 25%, 80 °C	No	52	SiO_2	0.13	0.16
4	F. Horikiri et al. [41]	GaN/GaN	TMAH, 25%, 85 °C	Yes	30	SiO_2	0.1-2	—

As shown in Figure 6, sample2 has a star-shaped pattern with 24 identical GaN fingers with 250 nm width and 2.3 µm thickness separated by 15° angles. These GaN fingers were characterized after 30 min of wet etching in TMAH solution.

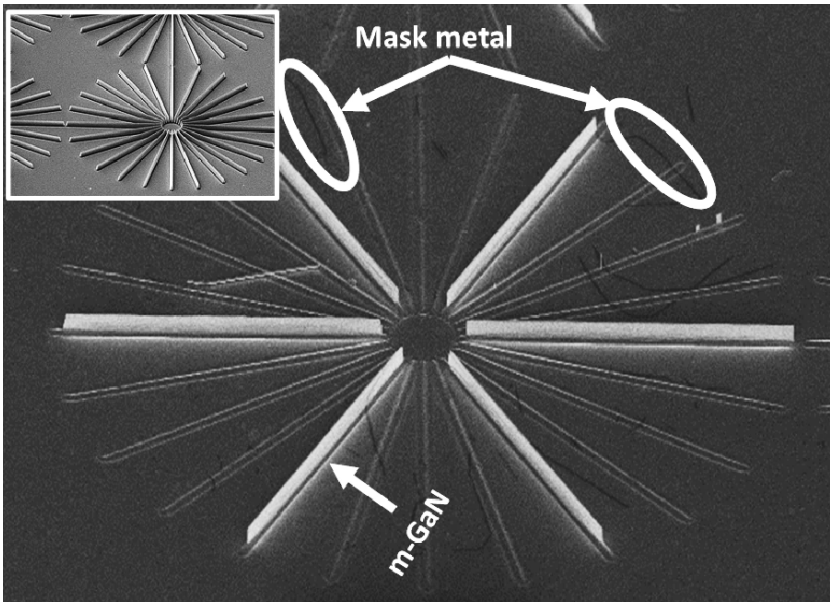


Figure 6. Star shape pattern after 30 min TMAH etching (insert: picture of the same pattern before TMAH etching).

Figure 6 clearly shows that only m-GaN oriented fingers remain after 30 min TMAH etching. Meanwhile, all the other Fins have been etched. In this experiment it's highlighted that the GaN m-plane is less etched in TMAH solution than other GaN crystallographic planes [33].

4. Conclusions

This work proposes an orientation determination procedure for crystallographic wet etching of a-GaN and m-GaN planes. This pre-alignment procedure is very helpful for the GaN wafers where the exact in-plane crystal orientation is not well identified as for diced coupons. By using the proposed procedure, the m and a-GaN planes are precisely identified. An optimized TMAH 25%, 85 °C and UV-assisted recipe has been used to engineer both a-and m-GaN oriented Fin channels. The etching of m-GaN crystal plane reveals smoother and more stable channel sidewalls than those on a-GaN oriented Fins. The Cuboids at the bottom of the GaN fingers are also investigated. Several tests have been performed and still need more investigation to deeply understand the origin of these Cuboids created during the TMAH etching. The impact of UV-light utilization on m and a-GaN planes etching rates in TMAH solution has been investigated. The m-GaN etching rate is enhanced from 0.69 to 1.09 nm/min with UV-light utilization. In the a-GaN plane, the UV-light enhances the etching rate from 2.94 to 4.69 nm/min. Finally, the obtained results in this work are innovative and will offer more knowledge about a- and m-GaN planes etching mechanisms which is a key step in the vertical GaN FinFET fabrication process.

Author Contributions: Writing—original draft preparation, N.A.T.; writing—review and editing, N.A.T., C.R., H.M., A.S., Y.C., E.F., F.M., C.S., L.-V.P., F.T.; visualization, N.A.T., H.M.; supervision, H.M.; project administration, H.M.; funding acquisition, H.M.; All authors have read and agreed to the published version of the manuscript.

Funding: This research funded by Fonds de Recherches du Quebec—Nature, Technologies (FRQNT), the Natural Sciences and En-gineering Research Council of Canada (NSERC), French technology facility network RENATECH, French National Research Agency (ANR) through the project C-Pi-GaN, and the "Investissements d'Avenir"program GaNeX (ANR-11-LABX-0014).

Data Availability Statement: The data presented in this study are new and have not been previously published.

Acknowledgments: This work was supported by Fonds de Recherches du Quebec—Nature, Technologies (FRQNT), the Natural Sciences and Engineering Research Council of Canada (NSERC), French technology facility network RENATECH, French National Research Agency (ANR) through the project C-Pi-GaN, and the "Investissements d'Avenir"program GaNeX (ANR-11-LABX-0014).

Conflicts of Interest: The author declares no conflict of interest.

References

1. Li, R.; Cao, Y.; Chen, M.; Chu, R. 600 V/1.7—Normally-off GaN vertical trench metal–oxide–semiconductor field-effect transistor. *IEEE Electron Device Lett.* **2016**, *37*, 1466–1469. [CrossRef]
2. Conole, G.; Hall, M.; Smith, S. Enabling professional communication for practitioners across Europe. *Int. Conf. Comput. Educ. Proc.* **2003**, *47*, 659–660. [CrossRef]
3. Baliga, B. Power semiconductor device figure of merit for high-frequency applications. *IEEE Electron Device Lett.* **1989**, *10*, 455–457. [CrossRef]
4. Baliga, B.J. Gallium nitride devices for power electronic applications. *Semicond. Sci. Technol.* **2013**, *28*. [CrossRef]
5. Ma, C.-T.; Gu, Z.-H. Review of GaN HEMT Applications in Power Converters over 500 W. *Electronics* **2019**, *8*, 1401. [CrossRef]
6. Tsao, J.Y.; Chowdhury, S.; Hollis, M.A.; Jena, D.; Johnson, N.M.; Jones, K.A.; Kaplar, R.J.; Rajan, S.; Van de Walle, C.G.; Bellotti, E.; et al. Ultrawide-Bandgap Semiconductors: Research Opportunities and Challenges. *Adv. Electron. Mater.* **2018**, *4*. [CrossRef]
7. Amano, H.; Baines, Y.; Beam, E.; Borga, M.; Bouchet, T.; Chalker, P.R.; Charles, M.; Chen, K.J.; Chowdhury, N.; Chu, R.; et al. The 2018 GaN power electronics roadmap—IOP science. *J. Phys. D Appl. Phys. Top.* **2018**, *51*, 3001.
8. Chowdhury, S.; Mishra, U.K. Lateral and Vertical Transistors Using the AlGaN/GaN Heterostructure. *IEEE Trans. Electron Devices* **2013**, *60*, 3060–3066. [CrossRef]
9. Chakroun, A.; Jaouad, A.; Soltani, A.; Arenas, O.; Aimez, V.; Ares, R.; Maher, H. AlGaN/GaN MOS-HEMT Device Fabricated Using a High Quality PECVD Passivation Process. *IEEE Electron Device Lett.* **2017**, *38*, 779–782. [CrossRef]
10. Cheney, D.J.; Douglas, E.A.; Liu, L.; Lo, C.-F.; Gila, B.P.; Ren, F.; Pearton, S.J. Degradation Mechanisms for GaN and GaAs High Speed Transistors. *Materials* **2012**, *5*, 2498–2520. [CrossRef]
11. Ben-Yaacov, I.; Seck, Y.-K.; Mishra, U.K.; Denbaars, S. AlGaN/GaN current aperture vertical electron transistors with regrown channels. *J. Appl. Phys.* **2004**, *95*, 2073–2078. [CrossRef]

12. Huang, H.; Li, F.; Sun, Z.; Sun, N.; Zhang, F.; Cao, Y.; Zhang, H.; Tao, P. Gallium Nitride Normally-Off Vertical Field-Effect Transistor Featuring an Additional Back Current Blocking Layer Structure. *Electronics* **2019**, *8*, 241. [CrossRef]
13. Xiao, M.; Gao, X.; Palacios, T.; Zhang, Y. Leakage and breakdown mechanisms of GaN vertical power FinFETs. *Appl. Phys. Lett.* **2019**, *114*, 163503. [CrossRef]
14. Zubair, A.; Perozek, J.; Niroula, J.; Aktas, O.; Odnoblyudov, V.; Palacios, T. First Demonstration of GaN Vertical Power FinFETs on Engineered Substrate. In Proceedings of the 2020 Device Research Conference (DRC), Columbus, OH, USA, 21–24 June 2020; pp. 1–2.
15. Li, W.; Chowdhury, S. Design and fabrication of a 1.2 kV GaN-based MOS vertical transistor for single chip normally off operation. *Phys. Status Solidi Appl. Mater. Sci.* **2016**, *213*, 2714–2720. [CrossRef]
16. Abdul Khadar, R.M.; Liu, C.; Soleimanzadeh, R.; Matioli, E. Fully Vertical GaN-on-Si power MOSFETs. *IEEE Electron Device Lett.* **2019**, *40*, 443–446. [CrossRef]
17. Shibata, D.; Kajitani, R.; Ogawa, M.; Tanaka, K.; Tamura, S.; Hatsuda, T. 1.7 kV/1.0—Normally-off Vertical GaN Transistor on GaN substrate with Regrown p-GaN/AlGaN/GaN Semipolar Gate Structure. In Proceedings of the 2016 IEEE International Electron Devices Meeting (IEDM), San Francisco, CA, USA, 3–7 December 2016; pp. 248–251.
18. Xiao, M.; Palacios, T.; Zhang, Y. ON-Resistance in Vertical Power FinFETs. *IEEE Trans. Electron Devices* **2019**, *66*, 3903–3909. [CrossRef]
19. Sokolovskij, R.; Sun, J.; Santagata, F.; Iervolino, E.; Li, S.; Zhang, G.; Sarro, P. Precision Recess of AlGaN/GaN with Controllable Etching Rate Using ICP-RIE Oxidation and Wet Etching. *Procedia Eng.* **2016**, *168*, 1094–1097. [CrossRef]
20. Shah, A.P.; Azizur Rahman, A.; Bhattacharya, A. Temperature-dependence of Cl_2/Ar ICP-RIE of polar, semipolar, and non-polar GaN and AlN following BCl_3/Ar breakthrough plasma. *J. Vac. Sci. Technol. A* **2020**, *38*, 013001. [CrossRef]
21. Zhu, K. Evolution of surface roughness of AlN and GaN induced by inductively coupled Cl_2/Ar plasma etching. *J. Appl. Phys.* **2004**, *95*, 4635–4641. [CrossRef]
22. Merlos, A.; Acero, M.C.; Bao, M.; Bausells, J.; Esteve, J. TMAH/IPA anisotropic etching characteristics. *Sens. Actuators A Phys.* **1993**, *37–38*, 737–743. [CrossRef]
23. Zhang, Y.; Sun, M.; Liu, Z.; Piedra, D.; Hu, J.; Gao, X.; Palacios, T. Trench formation and corner rounding in vertical GaN power devices. *Appl. Phys. Lett.* **2017**, *110*, 193506. [CrossRef]
24. Wei, T.; Duan, R.; Wang, J.; Li, J.; Huo, Z.; Yang, J.; Zeng, Y. Microstructure and optical properties of non-polar m-plane GaN films grown on m-plane sapphire by hydride vapor phase epitaxy. *Jpn. J. Appl. Phys.* **2008**, *47*, 3346–3349. [CrossRef]
25. Dannecker, K.; Baringhaus, J. Fabrication of crystal plane oriented trenches in gallium nitride using SF6 + Ar dry etching and wet etching post-treatment. *J. Vac. Sci. Technol. A* **2020**, *38*, 043204. [CrossRef]
26. Tsai, M.C.; Leung, B.; Balakrishnan, G.; Wang, G.T. Understanding and Predicting GaN Anisotropic Wet Etch Facet Evolution Practical Motivation Etch rates of c-plane GaN for various chemistries. In Proceedings of the Electronic Material Conference, Zhengzhou, China, 11–12 April 2016; pp. 1–26.
27. Pearton, S.; Shul, R.J.; Ren, F. A Review of Dry Etching of GaN and Related Materials. *MRS Internet J. Nitride Semicond. Res.* **2000**, *5*, 1–38. [CrossRef]
28. Tautz, M.; Díaz, D.D. Wet-Chemical Etching of GaN: Underlying Mechanism of a Key Step in Blue and White LED Production. *ChemistrySelect* **2018**, *3*, 1480–1494. [CrossRef]
29. Zhang, Y.; Sun, M.; Wong, H.Y.; Lin, Y.; Srivastava, P.; Hatem, C.; Azize, M.; Piedra, D.; Yu, L.; Sumitomo, T.; et al. Origin and Control of OFF-State Leakage Current in GaN-on-Si Vertical Diodes. *IEEE Trans. Electron Devices* **2015**, *62*, 2155–2161. [CrossRef]
30. Fatahilah, M.F.; Strempel, K.; Yu, F.; Vodapally, S.; Waag, A.; Wasisto, H.S. 3D GaN nanoarchitecture for field-effect transistors. *Micro Nano Eng.* **2019**, *3*, 59–81. [CrossRef]
31. Hwang, J.; Ho, K.; Hwang, Z.; Hung, W.; Lau, K.M.; Hwang, H.-L. Efficient wet etching of GaN and p-GaN assisted with chopped UV source. *Superlattices Microstruct.* **2004**, *35*, 45–57. [CrossRef]
32. Powell, R.J.; Derbenwick, G.F. Vacuum ultraviolet radiation effects in SiO 2(Vacuum UV irradiation of silicon dioxide, discussing positive charging for photon energies above threshold for electron-hole pair creation). *IEEE Trans. Nucl. Sci.* **1971**, *18*, 99–105. [CrossRef]
33. Jun-Lin, L.; Jian-Li, Z.; Guang-Xu, W.; Chun-Lan, M.; Long-Quan, X.; Jie, D.; Quan, Z.-J.; Wang, X.-L.; Pan, S.; Zheng, C.-D. Status of GaN-based green light-emitting diodes. *Chin. Phys. B* **2015**, *24*, 7804–7810.
34. Kim, K.W.; Jung, S.D.; Kim, D.S.; Kang, H.S.; Im, K.S.; Oh, J.J.; Ha, J.-B.; Shin, J.-K.; Lee, J.H. Effects of TMAH treatment on device performance of normally off Al_2O_3/GaN MOSFET. *IEEE Electron Device Lett.* **2011**, *32*, 1376–1378. [CrossRef]
35. Leung, B.; Tsai, M.C.; Li, C.; Liu, S.; Figiel, J.J.; Allerman, A.A.; Crawford, M.; Balakrishnan, G.; Brueck, S.; Wang, G.T. *Crystallographic Etching of GaN: Fundamentals and Applications to Nanostructure Synthesis*; Sandia National Lab. (SNL-NM): Albuquerque, NM, USA, 2011.
36. Sun, Y.; Kang, X.; Zheng, Y.; Wei, K.; Li, P.; Wang, W.; Liu, X.; Zhang, G. Optimization of Mesa Etch for a Quasi-Vertical GaN Schottky Barrier Diode (SBD) by Inductively Coupled Plasma (ICP) and Device Characteristics. *Nanomaterials* **2020**, *10*, 657. [CrossRef] [PubMed]
37. Lee, S.; Mishkat-Ul-Masabih, S.; Leonard, J.T.; Feezell, D.F.; Cohen, D.A.; Speck, J.S.; Nakamura, S.; DenBaars, S.P. Smooth and selective photo-electrochemical etching of heavily doped GaN:Si using a mode-locked 355 nm mi-crochip laser. *Appl. Phys. Express* **2017**, *10*, 10–13. [CrossRef]

38. Stocker, D.A.; Schubert, E.F.; Redwing, J.M. Crystallographic wet chemical etching of GaN. *Appl. Phys. Lett.* **1998**, *73*, 2654–2656. [CrossRef]
39. Zhuang, D.; Edgar, J. Wet etching of GaN, AlN, and SiC: A review. *Mater. Sci. Eng. R Rep.* **2005**, *48*, 1–46. [CrossRef]
40. Chen, W.; Lin, J.; Hu, G.; Han, X.; Liu, M.; Yang, Y.; Wu, Z.; Liu, Y.; Zhang, B. GaN nanowire fabricated by selective wet-etching of GaN micro truncated-pyramid. *J. Cryst. Growth* **2015**, *426*, 168–172. [CrossRef]
41. Horikiri, F.; Fukuhara, N.; Ohta, H.; Asai, N.; Narita, Y.; Yoshida, T.; Mishima, T.; Toguchi, M.; Miwa, K.; Sato, T. Simple wet-etching technology for GaN using an electrodeless photo-assisted electrochemical reaction with a luminous array film as the UV source. *Appl. Phys. Express* **2019**, *12*, 031003. [CrossRef]